



ELSEVIER

Contents lists available at ScienceDirect

Data in Brief

journal homepage: www.elsevier.com/locate/dib

Data Article

Lagrangian and Eulerian dataset of the wake downstream of a smooth cylinder at a Reynolds number equal to 3900

Ali Rahimi Khojasteh^{a,*}, Sylvain Laizet^b, Dominique Heitz^a, Yin Yang^a

^a INRAE, OPAALE, 17 avenue de Cucillé, Rennes 35044, France

^b Turbulence Simulation Group, Department of Aeronautics, Imperial College London, Exhibition Road, London SW7 2AZ, United Kingdom

ARTICLE INFO

Article history:

Received 25 August 2021

Revised 12 December 2021

Accepted 13 December 2021

Available online xxx

Keywords:

Lagrangian particle trajectory

Direct Numerical Simulation

Synthetic particle transport

Turbulent wake flow

ABSTRACT

The dataset contains Eulerian velocity and pressure fields, and Lagrangian particle trajectories of the wake flow downstream of a smooth cylinder at a Reynolds number equal to 3900. An open source Direct Numerical Simulation (DNS) flow solver named *Incompact3d* was used to calculate the Eulerian field around the cylinder. The synthetic Lagrangian tracer particles were transported using a fourth-order Runge-Kutta scheme in time and trilinear interpolations in space. Trajectories of roughly 200,000 particles for two 3D sub-domains are available to the public. This dataset can be used as a test case for tracking algorithm assessment, exploring the Lagrangian physics, statistic analyses, machine learning, and data assimilation interests.

© 2021 Published by Elsevier Inc.

This is an open access article under the CC BY license

(<http://creativecommons.org/licenses/by/4.0/>)

* Corresponding author.

E-mail address: ali.rahimi-khojasteh@inrae.fr (A.R. Khojasteh).<https://doi.org/10.1016/j.dib.2021.107725>

2352-3409/© 2021 Published by Elsevier Inc. This is an open access article under the CC BY license

(<http://creativecommons.org/licenses/by/4.0/>)

1 Specifications Table

Subject	Physics Engineering
Specific subject area	4D Particle Tracking Velocimetry (4D-PTV) Lagrangian Particle Tracking (LPT) Direct Numerical Simulation (DNS)
Type of data	Text file
How data were acquired	Direct Numerical Simulation (DNS) Synthetic particle transport
Data format	Raw
Parameters for data collection	The Eulerian velocity and pressure fields as well as the Lagrangian trajectories were collected for every 10 and 1 DNS time steps in sub-domain 1 and sub-domain 2, respectively.
Description of data collection	The Eulerian dataset was computed by an open-source Direct Numerical Simulation (DNS) code, named <code>Incompact3d</code> . The Eulerian velocity and pressure snapshots of two sub-domains were collected in the Data INRAE repository [1]. Nearly 200,000 synthetic Lagrangian trajectories were transported and saved for each sub-domain.
Data source location	Institution: French National Institute for Agriculture, Food, and Environment (INRAE) City/Town/Region: Rennes Country: France
Data accessibility	Repository name: Data INRAE Direct URL to data: https://doi.org/10.15454/GLNRHK Instructions for accessing these data: Free access
Related research article	Ali Rahimi Khojasteh, Yin Yang, Dominique Heitz, and Sylvain Laizet, "Lagrangian coherent track initialization", Physics of Fluids 33, 095113 (2021) [2] https://doi.org/10.1063/5.0060644

2 Value of the Data

- 3 • Recent rapid development in time-resolved three-dimensional Particle Tracking Velocimetry
4 (4D-PTV) and Particle Image Velocimetry (PIV) studies arises a need to have ground truth
5 datasets. To this end, a reference dataset was generated from a highly-resolved Direct Nu-
6 merical Simulation (DNS).
- 7 • The data can be used by the PIV/PTV algorithm developers for assessment and validation
8 purposes, as well as by those interested in machine learning and data assimilation studies in
9 fluid mechanics. Moreover, scientists can benefit from the Eulerian and Lagrangian snapshots
10 in the dataset to explore the physics of turbulent wake flows.
- 11 • Four types of data including, Lagrangian trajectories, 3D velocity fields, 2D velocity snapshots,
12 and pressure fields, in two sub-domains are available in the repository. As listed in Table 1,
13 one or more types of data can be used depending on the application.

Table 1

Application of the current dataset in PIV / PTV community.

Dataset application	Lagrangian trajectory	3D velocity field	2D velocity snapshot	Pressure field	Target studies
4D-PTV algorithm assessment	✓	✗	✗	✗	[2–5]
Volumetric pressure from PTV	✓	✗	✗	✓	[6,7]
4D flow field reconstruction	✓	✓	✗	✗	[8]
Lagrangian physics	✓	✗	✗	✗	[9,10]
Machine learning	✓	✗	✓	✗	[11,12]
Eulerian physics	✗	✓	✓	✗	-
Data assimilation	✓	✓	✗	✓	[13]
CFD assessment	✗	✓	✗	✓	-
2D2C-2D3C-PIV	✓	✓	✗	✗	[14]
Tomo-PIV	✓	✓	✗	✗	[14,15]

- 14 • There is an open-access Lagrangian particle transport software package in the data repository
 15 if interested readers require tracer particle trajectories with different properties including
 16 particle concentrations, temporal scale, and noise level.

17 1. Data Description

18 A highly-resolved Direct Numerical Simulation (DNS) of the flow over a smooth cylinder at a
 19 subcritical Reynolds number 3900 (based on the diameter D of the cylinder and the free-stream
 20 velocity) was performed to generate the data. Double-precision Eulerian and Lagrangian fields
 21 for two sub-domains were collected, as shown in Fig. 1. The dimensions of Sub-domain 1 are
 22 $10D \times 8D \times 6D$. Data were saved every 10 DNS time steps for Sub-domain 1 due to online
 23 cloud storage limitation (saving every time step would have required roughly 30 Tb of storage
 24 per vortex shedding). 1000 snapshots were also collected for a smaller sub-domain with dimen-
 25 sions of $4D \times 2D \times 2D$ (i.e., Sub-domain 2) for every DNS time step. Sub-domain 2 is suitable

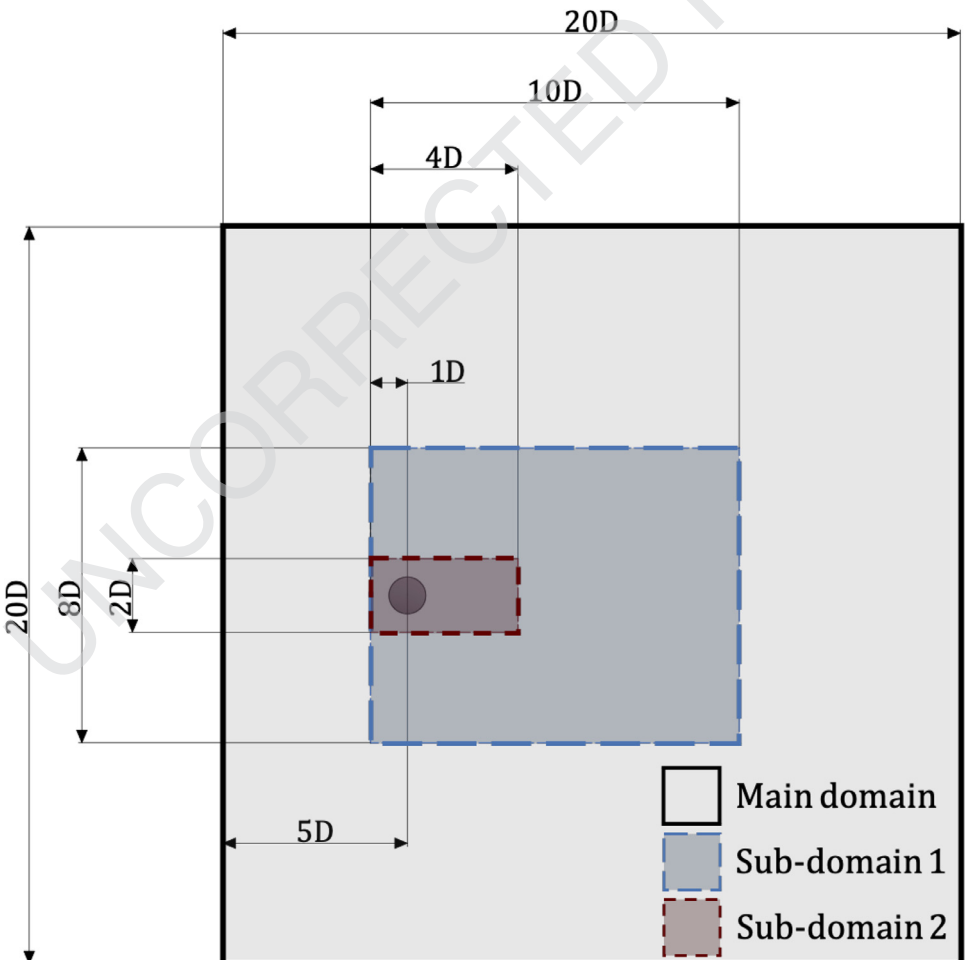


Fig. 1. Synthetic time scale selection with respect to recent similar wake flow experimental studies and different Reynolds numbers. Each symbol represents type of the experiment.

Table 2

Domain specification.

Domain	Dimension			Grid size			time step	Eulerian snapshot size
	x	y	z	n_x	n_y	n_z	dt	
Computation Domain	20D	20D	6D	1537	1025	256	0.00075 D/U_∞	12.9 Gb
Sub-domain 1	(4-14)D	(6-14)D	6D	769	777	256	0.00075 D/U_∞	4.8 Gb
Sub-domain 2	(4-8)D	(9-11)D	(2-4)D	308	328	87	0.0075 D/U_∞	256 Mb

26 for studies requiring the highest possible temporal resolution. Details of two sub-domains can
 27 be found in Table 2. One Eulerian snapshot of the current wake flow is shown in Fig. 2. For both
 28 sub-domains, Lagrangian trajectories are provided for roughly 200,000 synthetic particles. Three
 29 main categories are available in in the data repository, Sub-domain-1, Sub-domain-2, and Soft-
 30 ware. The snapshots are formatted in text (.txt) and collected in compressed files(.zip). There is
 31 no particular requirement for reading and opening the data. The naming format of each snap-
 32 shot is shown in Fig. 3. The Eulerian 3D snapshots are saved in vector formats. Therefore, it is
 33 necessary to extract them within three internal loops in xyz directions. The users also need to
 34 download the grid file separately to find the corresponding coordinates.

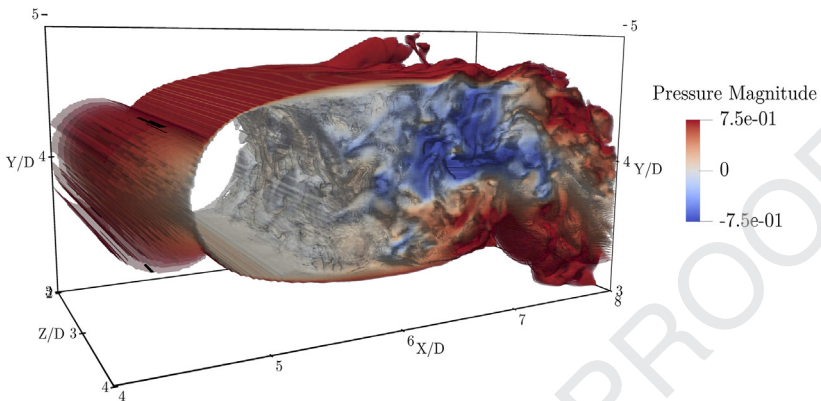
35 2. Experimental Design, Materials and Methods

36 The PIV/PTV community consistently requires synthetic datasets to assess and validate de-
 37 veloped image based methods. The EUROPIV Synthetic Image generator (SIG) developed a stan-
 38 dardised synthetic dataset framework for the PIV/PTV community [16]. SIG targeted three objec-
 39 tives including, algorithm performance assessment, algorithm sensitivity analysis as a function
 40 of characteristic parameters, and algorithm comparison. Characteristic parameters refer to par-
 41 ticle concentration (i.e., density), temporal scale, and noise ratio that can determine how the
 42 synthetic dataset is similar to a real experiment. Since then, by increasing capabilities of the
 43 PIV/PTV techniques, algorithm assessments constantly require datasets of flows with relatively
 44 complex and high gradient regions associated with 3D directional dynamics. That was the moti-
 45 vation to generate a database of Eulerian velocity and pressure fields with Lagrangian trajectories
 46 for the wake carrying complex flow motions downstream of a smooth cylinder. Applications of
 47 the current dataset can be summarised in Table 1.

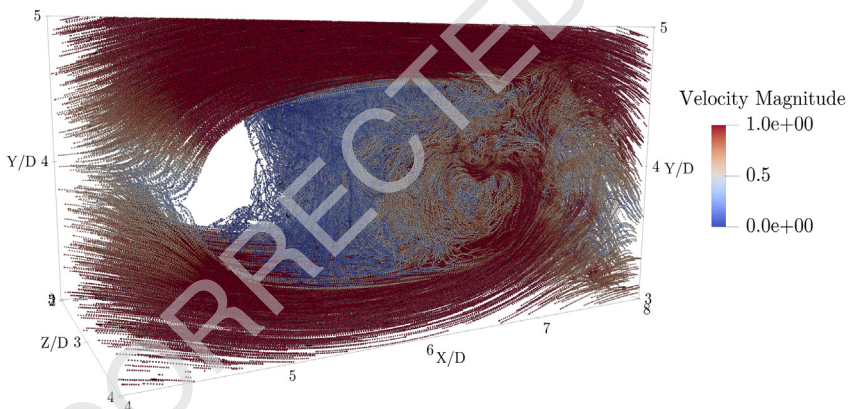
48 2.1. Eulerian method

49 The computations are carried out with the open-source flow solver named Incompact3d
 50 [17,18] based on sixth-order finite-difference compact schemes for the spatial discretisation on
 51 a Cartesian grid. Simplicity of the Cartesian grid offers the ability of implementing higher order
 52 spectral schemes for spatial discretisation. For the current simulation, the time advancement
 53 was performed with an explicit third-order Adams Bashforth scheme. The governing equations
 54 are solved with a fractional step method to treat the incompressibility constraint, which requires
 55 solving an additional projection step, the Poisson equation. This Poisson equation is fully solved
 56 in spectral space using three-dimensional Fast Fourier Transforms (FFTs). In the present work,
 57 the smooth cylinder is modelled using a customised immersed boundary method (IBM) with an
 58 artificial flow inside the cylinder to ensure the smoothness of the velocity field while imposing
 59 a no-slip boundary condition at the cylinder. More details about the flow solver can be found in
 60 Laizet and Lamballais [17]. Incompact3d is built with a powerful 2D domain decomposition
 61 for simulations on super-computers. The computational domain is split into a number of sub-
 62 regions (pencils) which are each assigned to an MPI process. The derivatives and interpolations

a) Pressure Iso_Surface



b) Lagrangian Trajectory



c) Q criterion Iso_Surface

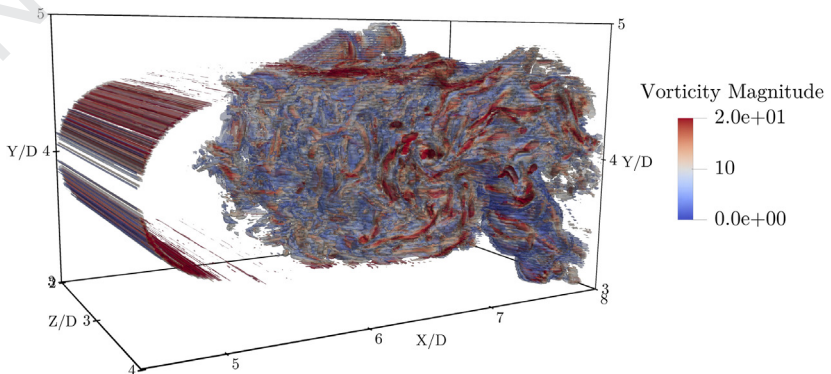


Fig. 2. Snapshot view of Sub-domain 2: (a), Pressure iso-surface coloured by the magnitude of pressure; (b), Lagrangian trajectories of 20,000 particles after 1000 DNS time step coloured by the velocity magnitude; (c), Q criterion representation of the Eulerian flow structures coloured by the vorticity magnitude.



Parameter: U V W P 2D	Domain: sub_domain_1 sub_domain_2	Timestep: 1,2,3,...	Tag: U_sub_domain_1 . . .
---------------------------------------------	------------------------------------------------	-------------------------------	----------------------------------------------

Fig. 3. The naming format of each snapshot in the data repository.

63 in the x-direction (y-direction, z-direction) are performed in X-pencils (Y-pencils, Z-pencils), re-
 64 spectively. The 3D FFTs required by the Poisson solver are also broken down as series of 1D
 65 FFTs computed in one direction at a time. Global transpositions to switch from one pencil to
 66 another are performed with the MPI command `MPI_ALLTOALL(V)`. `Incompact3d` can scale
 67 well with up to hundreds of thousands of MPI processes for simulations with several billion grid
 68 nodes [18]. Inflow/outflow boundary conditions are implemented along the streamwise direction
 69 with free-slip and periodic boundary conditions along the vertical and spanwise directions, re-
 70 spectively. The simulation was performed on nearly 4×10^{10} grid points (see Table 2). The grid
 71 was uniform in the streamwise and spanwise directions, while a non-uniform grid was used
 72 in the vertical direction, with a grid refinement towards the centre of the cylinder. The finest
 73 grid size in the vertical direction was $\Delta y_{\min} = 0.00563D$. The dimensional DNS time step was
 74 $0.00075D/U_{\infty}$ (where U_{∞} is the free-stream velocity). It takes 6667 DNS time steps to simulate
 75 one vortex shedding. It should also be mentioned that 1333 DNS time steps correspond to one
 76 integral temporal scale D/U_{∞} .

77 2.2. Lagrangian method

78 2.2.1. Particle transport

79 The Johns Hopkins Turbulence Database (JHTDB) generated from DNS has been employed
 80 widely for the quantitative performance assessment of PIV/PTV algorithms [19]. JHTDB contains
 81 nine multi-terabyte datasets in turbulent cases such as homogeneous isotropic turbulence (HIT)
 82 and channel flows. The current study brings added value to the available databases [16,19,20] by
 83 providing a case in the wake flow. Numerous complexities occur in the wake behind the cylin-
 84 der at subcritical Reynolds number, which can be a challenging test case for quantitative assess-
 85 ments.

86 In the present dataset, synthetic particles were transported using a conventional fourth-order
 87 Runge-Kutta scheme in time. The Lagrangian velocities of the synthetic particles were calculated
 88 by trilinear spatial interpolations over eight nearest neighbour grid points. To mimic the real
 89 experimental condition, three characteristic parameters, temporal scale, particle concentration,
 90 and noise ratio must be defined. Depending on the desired temporal scale, the synthetic time
 91 step can be calculated by knowing that the DNS time step of the current dataset is roughly
 92 20 times smaller than the Kolmogorov temporal scale. The desired temporal scale should be

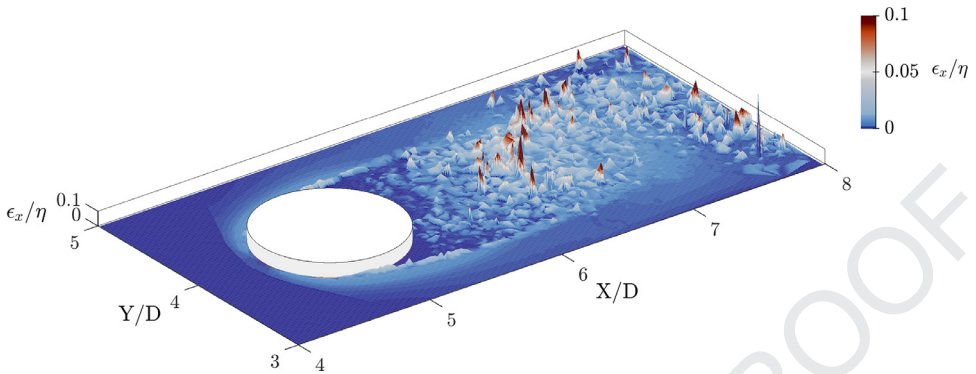


Fig. 4. 2D map of the non dimensional position error of Lagrangian transport computed every 10 DNS time step after 1000 time steps and after an average in the spanwise direction.

93 defined based on experimental hardware facilities, such as the illumination pulse rate or the
 94 camera frequency. The particle concentration also can be computed based on the number of
 95 particles per Kolmogorov length scale ($pp\eta^3$). The Kolmogorov length scale is almost 2.8 times
 96 smaller than the average grid size in the vertical direction for the current dataset. In a real
 97 experiment, the achievable spatial resolution is highly limited by the particle seeding system
 98 and the PIV/PTV algorithm performance. Therefore, an appropriate number of synthetic particles
 99 in the domain can be selected depending on the desired spatial resolution. An open-access tracer
 100 particle transport software package in MATLAB graphical user interface (GUI) is available as an
 101 additional tool in the data repository. Interested users can create tracer particle trajectories with
 102 different properties including particle concentrations up to the DNS spatial resolution, temporal
 103 scale up to the DNS time scale, and noise level.

104 2.2.2. Particle transport accuracy

105 A comparison was made between the transport of particles at every 10 DNS time step (i.e.,
 106 temporal scale of Sub-domain 1) with the transport of particles at every DNS time step in Sub-
 107 domain 2, to quantify the uncertainty level of trajectories in Sub-domain 1. As a result, the mean
 108 deviation of the trajectories between two temporal scales after 1000 DNS time steps in the larger
 109 domain is equal to 3.28η , with η the Kolmogorov spatial scale. The standard deviation of posi-
 110 tion error is $\sigma_\epsilon = 0.017\eta$. Fig. 4 shows a 2D map of the non-dimensional position deviation ϵ/η
 111 between two temporal scales averaged in the spanwise direction. Therefore, it is recommended
 112 to use the data from Sub-domain 2 for studies requiring accurate trajectories inside the wake
 113 region, while the data from Sub-domain 1 are better suited for studies focusing on large scale
 114 motions.

115 Ethics Statement

116 This study did not conduct experiments involving humans and animals.

117 Declaration of Competing Interest

118 The authors declare that they have no known competing financial interests or personal rela-
 119 tionships that could have appeared to influence the work reported in this paper.

120 CRediT Author Statement

121 **Ali Rahimi Khojasteh:** Conceptualization, Methodology, Investigation, Visualization, Writing – original draft; **Sylvain Laizet:** Methodology, Investigation, Writing – review & editing; **Dominique Heitz:** Methodology, Supervision, Writing – review & editing; **Yin Yang:** Methodology, Writing – review & editing.

125 Acknowledgment

126 The authors would like to thank EPSRC in the UK for the computational time made available
127 on the UK supercomputing facility ARCHER2 via the UK Turbulence Consortium (EP/R029326/1).

128 Supplementary Material

129 Supplementary material associated with this article can be found in the online version at
130 doi:[10.1016/j.dib.2021.107725](https://doi.org/10.1016/j.dib.2021.107725).

131 References

- 132 [1] A. R. Khojasteh, S. Laizet, D. Heitz, Y. Yang, Lagrangian and Eulerian dataset of flow over a circular cylinder at
133 Reynolds number 3900, Data INRAE (2021a). 10.15454/GLNRHK.
- 134 [2] A.R. Khojasteh, Y. Yang, D. Heitz, S. Laizet, Lagrangian coherent track initialization, Phys. Fluids 33 (9) (2021b)
135 095113, doi:[10.1063/5.0060644](https://doi.org/10.1063/5.0060644).
- 136 [3] D. Schanz, S. Gesemann, A. Schröder, Shake-the-box: Lagrangian particle tracking at high particle image densities,
137 Exp. Fluids 57 (2016) 1–27, doi:[10.1007/s00348-016-2157-1](https://doi.org/10.1007/s00348-016-2157-1).
- 138 [4] S. Tan, A. Salibindla, A.U.M. Masuk, R. Ni, Introducing OpenLPT: new method of removing ghost particles and high-
139 concentration particle shadow tracking, Exp. Fluids 61 (2) (2020) 1–16, doi:[10.1007/s00348-019-2875-2](https://doi.org/10.1007/s00348-019-2875-2).
- 140 [5] A.R. Khojasteh, D. Heitz, Y. Yang, L. Fiabane, Particle position prediction based on Lagrangian coherency for flow
141 over a cylinder in 4D-PTV, in: Proceedings of the 14th International Symposium on Particle Image Velocimetry,
142 Illinois, USA, 2021, pp. 1–9. <https://hal.inrae.fr/hal-03316123>.
- 143 [6] F. Huhn, A. Schröder, D. Schanz, S. Gesemann, P. Manovski, Estimation of time-resolved 3D pressure fields in an
144 impinging jet flow from dense Lagrangian particle tracking, in: Proceedings of the 18th International Symposium
145 on Flow Visualization, Zurich, Switzerland, 2018, pp. 1–14, doi:[10.3929/ethz-b-000279200](https://doi.org/10.3929/ethz-b-000279200).
- 146 [7] M. Bobrov, M. Hrebtov, V. Ivashchenko, R. Mullyadzhyanov, A. Seredkin, M. Tokarev, D. Zaripov, V. Dulin,
147 D. Markovich, Pressure evaluation from Lagrangian particle tracking data using a grid-free least-squares method,
148 Meas. Sci. Technol. 32 (084014) (2021) 1–14, doi:[10.1088/1361-6501/abf95c](https://doi.org/10.1088/1361-6501/abf95c). <https://iopscience.iop.org/article/10.1088/1361-6501/abf95c/meta>
- 149 [8] J.F. Schneiders, F. Scarano, Dense velocity reconstruction from tomographic PTV with material derivatives, Exp. Fluids
150 57 (9) (2016) 1–22, doi:[10.1007/s00348-016-2225-6](https://doi.org/10.1007/s00348-016-2225-6).
- 151 [9] F.A.C. Martins, A. Sciacchitano, D.E. Rival, Detection of vortical structures in sparse Lagrangian data using coherent-
152 structure colouring, Exp. Fluids 62 (2021) 1–15, doi:[10.1007/s00348-021-03135-5](https://doi.org/10.1007/s00348-021-03135-5).
- 153 [10] A. Schröder, D. Schanz, D. Michaelis, C. Cierpka, S. Scharnowski, C.J. Kähler, Advances of PIV and 4D-PTV “shake-
154 the-box” for turbulent flow analysis – the flow over periodic hills, Flow, Turbul. Combust. 95 (2-3) (2015) 193–209,
155 doi:[10.1007/s10494-015-9616-2](https://doi.org/10.1007/s10494-015-9616-2).
- 156 [11] Y. Gim, D.K. Jang, D.K. Sohn, H. Kim, H.S. Ko, Three-dimensional particle tracking velocimetry using shallow neural
157 network for real-time analysis, Exp. Fluids 61 (2) (2020) 1–8, doi:[10.1007/s00348-019-2861-8](https://doi.org/10.1007/s00348-019-2861-8).
- 158 [12] D. Puzryev, K. Harth, T. Trittel, R. Stannarius, Machine learning for 3D particle tracking in granular gases, Micro-
159 graphy Sci. Technol. 32 (5) (2020) 897–906, doi:[10.1007/s12217-020-09800-4](https://doi.org/10.1007/s12217-020-09800-4).
- 160 [13] V.J. Jeon, M. Müller, D. Michaelis, B. Wieneke, Data assimilation-based flow field reconstruction from particle tracks
161 over multiple time steps, in: Proceedings of the 13th International Symposium on Particle Image Velocimetry, 2019,
162 pp. 1–8.
- 163 [14] G.E. Elsinga, F. Scarano, B. Wieneke, B.W. Van Oudheusden, Tomographic particle image velocimetry, Exp. Fluids 41
164 (2006) 933–947, doi:[10.1007/s00348-006-0212-z](https://doi.org/10.1007/s00348-006-0212-z).
- 165 [15] S. Discetti, F. Coletti, Volumetric velocimetry for fluid flows, Meas. Sci. Technol. 29 (4) (2018) 1–26, doi:[10.1088/1361-6501/aaa571](https://doi.org/10.1088/1361-6501/aaa571).
- 166 [16] B. Lecordier, J. Westerweel, The EUROPIV Synthetic Image Generator (S.I.G.), in: Particle Image Velocimetry: Recent
167 Improvements, 2004, pp. 145–161, doi:[10.1007/978-3-642-18795-7_11](https://doi.org/10.1007/978-3-642-18795-7_11).
- 168 [17] S. Laizet, E. Lamballais, High-order compact schemes for incompressible flows: a simple and efficient method with
169 quasi-spectral accuracy, J. Comput. Phys. 228 (2009) 5989–6015, doi:[10.1016/j.jcp.2009.05.010](https://doi.org/10.1016/j.jcp.2009.05.010).
- 170 [18] S. Laizet, N. Li, Incompact3d: A powerful tool to tackle turbulence problems with up to O(105) computational cores,
171 Int. J. Numer. Methods Fluids 67 (2011) 1735–1757, doi:[10.1002/fld.2480](https://doi.org/10.1002/fld.2480).

- 174 [19] Y. Li, E. Perlman, M. Wan, Y. Yang, C. Meneveau, R. Burns, S. Chen, A. Szalay, G. Eyink, A public turbulence database
175 cluster and applications to study Lagrangian evolution of velocity increments in turbulence, *J. Turbul.* 9 (31) (2008)
176 1–29, doi:[10.1080/14685240802376389](https://doi.org/10.1080/14685240802376389).
- 177 [20] B. Leclaire, I. Mary, C. Liauzun, S. Péron, A. Sciacchitano, A. Schröder, P. Cornic, F. Champagnat, First challenge on
178 Lagrangian particle tracking and data assimilation: datasets description and planned evolution to an open online
179 benchmark, in: *Proceedings of the 14th International Symposium on Particle Image Velocimetry*, Illinois, USA, 2021,
180 pp. 1–2. https://w3.onera.fr/first_lpt_and_da_challenge/.

UNCORRECTED PROOF